Translational Oncology 15 (2022) 101258

Contents lists available at ScienceDirect

Translational Oncology

journal homepage: www.elsevier.com/locate/tranon

Original Research

Dual roles of AMAP1 in the transcriptional regulation and intracellular trafficking of carbonic anhydrase IX

Mei Horikawa [a], Hisataka Sabe [a,*], Yasuhito Onodera [a,b,*]

[a] Department of Molecular Biology, Faculty of Medicine and Graduate School of Medicine, Hokkaido University, N15W7 Kita-ku, Sapporo, Hokkaido 060-8638, Japan
[b] Global Center for Biomedical Science and Engineering, Faculty of Medicine, Hokkaido University, N15W7 Kita-ku, Sapporo, Hokkaido 060-8638, Japan

ARTICLE INFO

Keywords:
CA9
ASAP1
Protein kinase D2
PIAS3
HIF1A

ABSTRACT

Background: The cell-surface enzyme carbonic anhydrase IX (CAIX/CA9) promotes tumor growth, survival, invasion, and metastasis, mainly via its pH-regulating functions. Owing to its tumor-specific expression, CAIX-targeting antibodies/chemicals are utilized for therapeutic and diagnostic purposes. However, mechanisms of CAIX trafficking, which affects such CAIX-targeting modalities remain unclear. In this study, roles of the AMAP1-PRKD2 pathway, which mediates integrin recycling of invasive cancer cells, in CAIX trafficking were investigated.

Methods: Using highly invasive MDA-MB-231 breast cancer cells, the physical association and colocalization of endogenous proteins were analyzed by immunoprecipitation and immunofluorescence, protein/mRNA levels were quantified by western blotting/qPCR, and cell-surface transport and intracellular/extracellular pH regulation were measured by biotin-labeling and fluorescent dye-based assays, respectively. The correlation between mRNA levels and patients' prognoses was analyzed using a TCGA breast cancer dataset.

Results: AMAP1 associated with the CAIX protein complex, and they colocalized at the plasma membrane and tubulovesicular structures. AMAP1 knockdown reduced total/surface CAIX, induced its lysosomal accumulation and degradation, and affected intracellular/extracellular pH. PRKD2 knockdown excluded AMAP1 from the CAIX complex and reduced total CAIX in a lysosome-dependent manner. Unexpectedly, AMAP1 knockdown also reduced CAIX mRNA. AMAP1 interacted with PIAS3, which stabilizes HIF-1α, a transcriptional regulator of *CA9*. AMAP1 knockdown inhibited the PIAS3-HIF-1α interaction and destabilized the HIF-1α protein. High-*ASAP1* (AMAP1-encoding gene) together with high-*PIAS3* correlated with high-*CA9* and an unfavorable prognosis in breast cancer.

Conclusion: The AMAP1-PRKD2 pathway regulates CAIX trafficking, and modulates its total/surface expression. The AMAP1-PIAS3 interaction augments *CA9* transcription by stabilizing HIF-1α, presumably contributing to an unfavorable prognosis.

Introduction

The unlimited proliferation of cancer cells and their metabolic changes substantially alter the metabolic microenvironment of tumor tissue. The reduced oxygen tension and the dependence of cancer cells on glycolysis for their macromolecule biosynthesis and signaling activities [1–3] result in the production of large amounts of lactic acid [4,5]. Although extracellular acidification promotes the drug resistance, invasion, metastasis, angiogenesis, and immune evasion of cancer cells [6,7], they still require a slightly alkaline intracellular pH for their proper cellular functions [8,9]. Various pH regulators play vital roles in cancer cells to avoid their intracellular acidification, and therefore, blocking such pH-regulating mechanisms has been considered a promising strategy for cancer therapy [10,11].

Carbonic anhydrase IX (CAIX/CA9), which is one of the main pH regulators in cancer cells [5,10,12], is a membrane-tethered enzyme with an extracellular catalytic domain. CAIX cooperates with diverse acid-base transporters on the cell surface to maintain intracellular pH,

Abbreviations: CAIX, carbonic anhydrase IX; AMAP1, A Multiple-domain Arf-GAP Protein 1; PRKD2, protein kinase D2; PIAS3, protein inhibitor of activated STAT3; HIF-1α, hypoxia inducible factor 1α; LAMP-1, lysosomal-associated membrane protein 1; ECM, extracellular matrix.

* Corresponding authors at: Department of Molecular Biology, Faculty of Medicine and Graduate School of Medicine, Hokkaido University, Sapporo, Hokkaido 060-8638, Japan.

E-mail addresses: sabeh@med.hokudai.ac.jp (H. Sabe), yonodera@med.hokudai.ac.jp (Y. Onodera).

https://doi.org/10.1016/j.tranon.2021.101258
Received 8 August 2021; Received in revised form 20 October 2021; Accepted 25 October 2021
Available online 3 November 2021

through its catalytic and noncatalytic domains, whereas it in turn induces extracellular acidification [13–15]. Besides supporting the growth and survival of cancer cells, CAIX also contributes to a broad range of malignant properties, such as signaling, epithelial-mesenchymal transition, invasion, and metastasis, mainly by its pH-regulating function [13,16–18]. A number of preclinical studies have shown that inhibition of the expression and/or functions of CAIX effectively blocks primary tumor growth and metastatic complication [13–15].

In various tissues and organs, CAIX is almost exclusively expressed in cancer cells, and no or very little expression is found in their normal counterparts [19,20]. The *CA9* promoter region contains a hypoxia responsive element, and thus its transcription is largely controlled by hypoxia-inducible factors (HIFs), which are often stabilized and increased in cancer cells by a hypoxic microenvironment and other genetic and/or metabolic alterations [21,22]. Studies using xenograft models and human tumor tissues have shown that hypoxic and/or acidic regions of primary tumors, metastatic lesions, and therapy-resistant tumors are associated with high CAIX expression [13, 20]. These expression patterns of CAIX are expected to be exploited for the diagnosis and treatment of cancers [20,23].

Current modalities targeting CAIX include 2 major strategies, namely, monoclonal antibodies and small molecules. In addition to such modalities targeting the enzymatic activity of CIAX, antibody-drug conjugates (ADC) and small molecule-drug conjugates (SMDC), which simultaneously ensure specificity and toxicity to cancer cells, are also being developed [20,24–26]. However, as the efficacy of antibody-based modalities can be affected by the intracellular trafficking of their target [27], optimization of these treatments requires elucidation of the roles and mechanisms of CAIX trafficking.

Although CAIX was shown to be constitutively internalized by clathrin-mediated endocytosis and to subsequently be recycled back to the plasma membrane [28], the molecular machinery involved in these processes have remained unknown. As the functions of CAIX require its localization on the cell surface, clarifying the molecular target in CAIX trafficking may not only improve the efficacy of existing CAIX-targeting modalities, but also contribute to the establishment of new treatment strategies.

We previously reported that the expression of multiple-domain Arf-GAP protein 1 (AMAP1), which is an effector of the small GTPase ARF6, is significantly increased in invasive breast cancers [29]. AMAP1 and ARF6 localize at invadopodia, and promote extracellular matrix (ECM) degradation, and the invasion and metastasis of cancer cells. [29,30]. AMAP1 forms a complex with β1-integrins to promote its recycling to the plasma membrane [31], which is essential for cancer invasion [32–34]. In this context, protein kinase D2 (PRKD2) acts as a molecular adaptor that links AMAP1 and β1-integrin [31,35]. Based on a recent report showing close similarities between CAIX and AMAP1, e.g., the association with β1-integrins and localization/function in invadopodia [17], we analyzed the physical and functional cooperation between CAIX and AMAP1, particularly focusing on the trafficking to the plasma membrane. Some of our *in vitro* findings were also validated using a dataset from The Cancer Genome Atlas (TCGA).

Materials and methods

Cells, chemicals and antibodies

All cell lines were obtained from American Type Culture Collection and cultured in a humidified CO_2 incubator at 37 °C. For MDA-MB-231 and BT549 cells, the culture medium was composed of equal volumes of DMEM (high glucose, SIGMA D5796) and RPMI 1640 (SIGMA R8758), supplemented with 10% fetal calf serum (FCS, HyClone), 5% NuSerum (Corning) and 2 mM L-glutamine, and the CO_2 concentration was set at 7.5%. For MDA-MB-436 cells, the culture medium was composed of L-15 medium supplemented with 10% FCS, 10 μg/mL insulin, and 16 μg/mL glutathione, and the CO_2 concentration was set at 0%. For 293T cells, the culture medium was composed of DMEM supplemented with 10% FCS, and the CO_2 concentration was set at 5%.

All chemicals used for the cell experiments were of the highest grade and/or validated as suitable for cell culture. Detailed descriptions of the chemicals, antibodies, and other materials are provided as Supplementary information.

siRNA transfection

The siRNA duplexes were chemically synthesized by Japan Bio Services. Their sequences are described in Supplementary information. Cells were transfected with siRNA at the same time as their seeding onto culture dishes using Lipofectamine™ RNAiMAX Transfection Reagent (Thermo), according to manufacturer's instruction ("reverse transfection" method). After 72 h, transfected cells were subjected to various assays.

Western blotting

Cellular protein extracts were isolated by directly adding NP-40 lysis buffer (1% NP-40, 150 mM NaCl, 20 mM Tris–HCl [pH 7.4], 5 mM EDTA) containing protease inhibitor cocktail set I (Calbiochem) to the cells after washing twice with ice-cold PBS. Then, the lysates containing cell debris were sonicated by Bioruptor UCD-250HSA (CosmoBio). The soluble fraction was isolated by centrifugation, and protein concentrations of the lysates were measured using DC™ Protein Assay kit (Bio-Rad). Protein extracts were separated by electrophoresis using Bolt™ gels (all blots for immunoprecipitation, and for PIAS3 (protein inhibitor of activated STAT3) and HIF-1α blots) (Thermo) or NuPage™ gels (CAIX, and PRKD2 blots) (Thermo), and then transferred to Immobilon-FL PVDF membranes (Millipore) using Mini Trans-Blot Cell (Bio-Rad). Membranes were blocked for 1 h in BlockPRO™ Protein-Free Blocking Buffer (Visual Protein) and probed overnight with primary antibodies for CAIX, AMAP1/ASAP1, PRKD2, PIAS3, HIF-1α or β-actin. Membranes were washed 3 times with TBST and incubated with Alexa fluor® 680-conjugated anti-mouse IgG and/or DyLight® 800 4X PEG-conjugated anti-rabbit IgG for 1 h. Membranes were analyzed using Odyssey® Infrared Imaging System (LI-COR Bioscience).

Immunoprecipitation

Lysates of MDA-MB-231 cells grown on collagen I-coated dishes were prepared as described in *Western blotting*, except that the sonication step was omitted. For immunoprecipitation (IP) using PRKD2-depleted cells, NH_4Cl (12.5 mM) and leupeptin (0.5 mM) were added 24 h before the lysis, to equalize CAIX protein with the control cells (see also Fig. 2I). For the co-IP of PIAS3 and HIF-1α, MG-132 (10 μM) was added to the cells transfected with control siRNA and AMAP1-targeting siRNA, 30 min and 6 h before the lysis, respectively, to stabilize and equalize the HIF-1α protein. Cellular lysates were then subjected to IP using the anti-CAIX antibody or anti-PIAS3 antibody, together with Protein A Sepharose™ 4 Fast Flow (GE Healthcare). Nonimmune rabbit IgG was used as a control. After gentle agitation at 4 °C for 2 h, the antigen-antibody complexes captured on Protein A beads were precipitated by centrifugation, and washed 3 times with ice-cold NP-40 lysis buffer. The precipitants and total lysates were analyzed by western blotting. For CAIX IP, membranes were probed overnight with the biotin-conjugated anti-CAIX antibody, followed by incubation with Dylight® 800-conjugated NeutrAvidin. The pulldown assay using GST-tagged proteins is described in Supplementary information.

Cell-surface labeling

MDA-MB-231 cells, together with the siRNA duplex-reagent complexes, were seeded onto 35-mm dishes coated with collagen I (see *siRNA transfection*). After 72 h, cells were washed twice with ice-cold

PBS containing 0.1 mM $CaCl_2$ and 1.0 mM $MgCl_2$ (PBS-CM). Then, ice-cold freshly prepared biotin-labeling solution (0.5 mg/mL sulfo-NHS-SS-biotin in PBS-CM) was added to the washed cells. Cells were incubated on ice for 30 min, with gentle shaking every 5 min. To quench the reaction, biotin-labeling solution was removed and replaced with 50 mM NH_4Cl in PBS-CM. Cells were incubated on ice for 10 min, and washed twice with ice-cold PBS. Cell lysates were prepared with NP-40 buffer supplemented with protease inhibitors (see *Western blotting*). Biotinylated proteins were collected from the lysates using NeutrAvidin Agarose beads (Pierce), and analyzed by western blotting. The antibody-based method for cell-surface labeling is described in Supplementary information.

Immunostaining and microscopy

For costaining of CAIX and AMAP1, MDA-MB-231 cells were seeded on glass-bottom dishes coated with collagen I, and fixed with methanol at −20 °C for 5 min, to preserve tubulovesicular structures containing AMAP1 [31]. For the costaining of CAIX and lysosomal-associated membrane protein 1 (LAMP-1), MDA-MB-231 cells were transfected with siRNAs (see *siRNA transfection*), and reseeded onto glass-bottom dishes 48 h after siRNA transfection with DMSO or 100 nM bafilomycin A1 in the medium. After 24 h, the cells were fixed by directly adding 2% paraformaldehyde to the medium and incubating at 37 °C for 10 min. Cells were washed twice with PBS, and refixed with methanol at −20 °C for 5 min. Then, the fixed cells were blocked for 1 h with MAXblock™ Blocking Medium (ActiveMotif), and probed for 1 h at room temperature (RT) with primary antibodies for CAIX, LAMP1, and AMAP1. Samples were washed 3 times with PBS, and incubated with Alexa fluor® 488-conjugated anti-mouse IgG and Alexa fluor® 568-conjugated anti-rabbit IgG, which were cross-adsorbed by the manufacturer and confirmed to produce no specific staining on their own, for 1 h at RT. After washing twice with PBS, the nuclei were stained with Hoechst 33342 for 10 min at RT. After washing with PBS, stained intracellular structures were imaged by fluorescence microscopy.

A Nikon Eclipse Ti microscope equipped with the A1R laser confocal module and NIS-Elements Imaging software (Nikon) was used to capture images of cells stained with CAIX and LAMP1. Staining of Hoechst 33342, Alexa fluor® 488, and Alexa fluor® 568 was detected using 400, 488, and 561 nm lasers combined with 450/50, 525/50, and 595/50 nm filters, respectively. A Leica TCS SP8 confocal laser-scanning microscope (Leica Microsystems) was used to capture images of cells stained with CAIX and AMAP1. Staining of Hoechst 33342, Alexa flor® 488, and Alexa fluor® 568 was detected using 405, 488, and 552 nm lasers combined with 410–498, 498–547, and 617–742 nm spectral detection, respectively.

Quantitative PCR

A total of 2.0×10^4 cells were seeded onto a single collagen I-coated well of a 96-well plate, and simultaneously transfected with siRNAs (targeting AMAP1 or PIAS3, or a negative control). Cell lysates were prepared 72 h after seeding, and reverse transcription was performed using Cell Amp™ Direct Probe RT-qPCR Kit (Takara). Quantitative PCR (qPCR) was performed with the obtained samples following the manufacturer's instructions. The following fluorescent qPCR probes were used: CA9 TaqMan® Gene Expression Assays, FAM-MGB (Hs00154208_m1); HIF1A TaqMan® Gene Expression Assays, FAM-MGB (Hs00153153_m1); ACTB TaqMan® Gene Expression Assays, VIC-MGB_PL (Hs99999903_m1). One of the FAM probes (for either *CA9* or *HIF1A*) was duplexed with the VIC probe (for *ACTB*), and the expression of *CA9* and *HIF1A* was normalized using that of *ACTB*. Assays were performed using LightCycler® 96 System (Roche).

Intracellular and extracellular acidification assays

MDA-MB-231 cells were transfected with siRNAs (see *siRNA transfection*). After 60 h, cells were collected using trypsin-EDTA solution, and 20,000 cells were seeded on 96 well plate coated with collagen I. To avoid the possible effects of CO_2 remaining in the plastic, the culture medium was switched to L-15 supplemented with 10% FCS, and cells were incubated in a CO_2-free, humidified incubator set at 37 °C for 12 h.

For the measurement of intracellular and extracellular acidification, pHrodo™ Green reagent (Thermo P35373) and Glycolysis Assay/Extracellular Acidification kit (Abcam ab197244) were used, respectively. Detailed methods are described in Supplementary information.

Statistics

All experiments were repeated at least 3 times. Normality of the datasets was validated by the Shapiro-Wilk test. Results are shown as mean values with error bars indicating the standard error of the mean (SEM). Statistical significance was analyzed by the two-tailed *t*-test, after the equality of variance was validated by the *F*-test. When multiple samples were compared, *P*-values were adjusted by the Holm-Sidak method.

Analysis of TCGA data

RNA-seq and clinical data of breast cancer patients ($n = 1075$) were obtained from TCGA (https://portal.gdc.cancer.gov/), based on the access approval given to subscribed users, which does not require an ethics statement. Samples were stratified by expression of either *ASAP1* (the gene encoding AMAP1) or *PIAS3*, with variable high/low thresholds. Samples with the top 15% *ASAP1* expression was further stratified by relative expression levels of *PIAS3*, with the variable high/low thresholds. The average *CA9* expression level (RSEM) was calculated in each group. Statistical significance was analyzed by the Brunner-Munzel test, which is independent of distributions and variances. For the analysis of the correlation of expression levels with prognosis, samples with top 15% *ASAP1* expression and top 25% *PIAS3* expression were categorized as the "*ASAP1*-high" and "*PIAS3*-high" groups, respectively. Survival curves were estimated based on the Kaplan-Meier method, and survival was compared by the log-rank test.

Results

AMAP1 interacts with CAIX and regulates its expression

To analyze the molecular interaction of CAIX with AMAP1, CAIX protein was immunoprecipitated from MDA-MB-231 cells. The CAIX immunoprecipitants contained AMAP1 (Fig. 1A), demonstrating the physical interaction of these 2 proteins. Essentially the same results were obtained using several different CAIX antibodies (Supplementary Fig. 1). Immunostaining of MDA-MB-231 cells showed the colocalization of AMAP1 and CAIX at the cell periphery and on vesicles (Fig. 1B, upper panels). These proteins also colocalized at tubulo-vesicular structures (Fig. 1B, lower panels), which resembles the colocalization pattern of AMAP1, PRKD2 and β1-integrin [31]. Their colocalizaton was also found at the perinuclear region (Fig. 1B), which appeared to be some type of membranous structure. Intriguingly, AMAP1 knockdown significantly reduced CAIX expression (Fig. 1C,D). The decrease in the surface expression of CAIX by AMAP1 knockdown was also confirmed by an antibody-based method (Fig. 1E,F), and a chemical labeling method (Fig. 1G,H). We then analyzed whether AMAP1 is essential for the functions of CAIX. We confirmed that CAIX knockdown reduced the extracellular acidification rate (Fig. 1I), whereas it increased intracellular acidity (Fig. 1J), as reported by others [36,37]. AMAP1 knockdown also resulted in similar effects (Fig. 1J,I), although to a lesser extent (for the mechanistic explanation, see Supplementary Fig. 5). These results

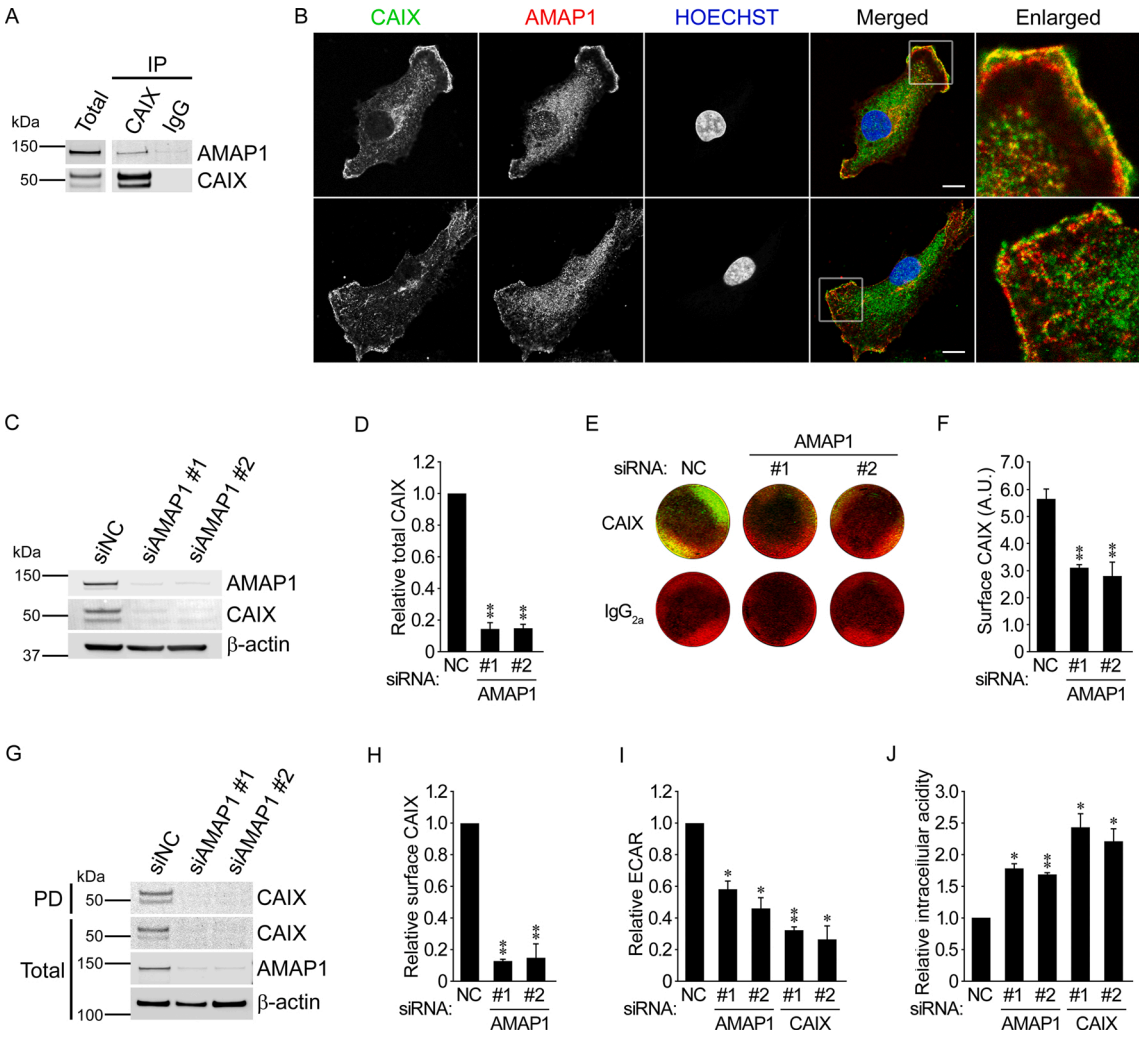

Fig. 1. AMAP1 regulates CAIX expression and cellular pH.
(A) CAIX was immunoprecipitated (IP) from MDA-MB-231 cell lysates. Nonimmune rabbit IgG was used as a control. Precipitants were analyzed by western blotting using the indicated antibodies. (B) MDA-MB-231 cells were immunostained using antibodies against CAIX (green) and AMAP1 (red). Nuclei were stained with Hoechst 33342 (blue). The right panels are enlarged images of the insets. Bars, 10 μm. (C–J) MDA-MB-231 cells were transfected with siRNAs targeting AMAP1 (siAMAP1) or negative control siRNA (siNC). Cell lysates were analyzed by western blotting using the indicated antibodies (C). Expression levels of CAIX, normalized to those of β-actin, were determined (D). Cells were fixed and stained with a CAIX antibody or an IgG_{2a} isotype control (green). Nuclei were stained with DRAQ5™ (red), and used as a surrogate of cell number (E). Surface CAIX level per cell was quantified based on staining intensities (F). Cells were surface-labeled with sulfo-NHS-SS-biotin, and biotinylated proteins were pulled down using NeutrAvidin beads (PD). Samples were analyzed by western blotting using the indicated antibodies (G). Surface expression levels of CAIX, normalized to total expression of β-actin, were determined (H). Extracellular acidification rate (ECAR, I) and intracellular acidity (J) were measured using fluorescent probes, and normalized to cell number determined by Hoechst 33342 staining. All graphs indicate the mean ± SEM from at least 3 independent experiments. * and **, $P < 0.05$ and $P < 0.005$, compared to the control samples, respectively.

suggest that AMAP1 plays essential roles in the maintenance of surface and/or total levels of CAIX to modulate its functions.

AMAP1 mediates the intracellular trafficking of CAIX

As AMAP1 regulates the recycling of cell-surface proteins such as β1-integrin and PD-L1 [31,38], and the inhibition of recycling often results in the lysosomal degradation of the unrecycled proteins [32,39], we speculated that AMAP1 also regulates the recycling of CAIX to the plasma membrane, and thus AMAP1 knockdown leads to the degradation of CAIX in lysosomes. Treatment of AMAP1-depleted cells with inhibitors of lysosomal degradation, including bafilomycin A1 (a V-ATPase inhibitor) (Fig. 2A,B), and leupeptin and NH_4Cl (lysosomal protease inhibitors) (Fig. 2C,D) partially rescued protein levels of CAIX, whereas the proteasome inhibitor MG-132, did not (Supplementary Fig. 2). The inhibition of lysosomes also increased the total protein levels of CAIX in control cells (Fig. 2A–D), indicating that a proportion of the CAIX protein undergoes constitutive lysosomal degradation. Consistently, immunofluorescence analysis showed that overall CAIX staining was very weak in AMAP1-depleted cells. The accumulation of CAIX in LAMP1-positive vesicular structures was occasionally observed, which became dominant when lysosomal degradation was inhibited (Fig. 2E, arrows). Such a staining pattern was not generally observed in control cells, although it was observed upon lysosomal inhibition. Intriguingly, the inhibition of lysosomes increased the surface-labeling of CAIX in control cells (Fig. 2F), indicating that a proportion of CAIX that escaped lysosomal degradation was translocated to the cell surface. On the other hand, AMAP1 knockdown largely abolished the increase in the surface-labeling of CAIX upon lysosomal inhibition (Fig. 2F). These results collectively suggest that the recycling back of CAIX to the cell surface, presumably from lysosomes or late endosomes, is mediated by AMAP1.

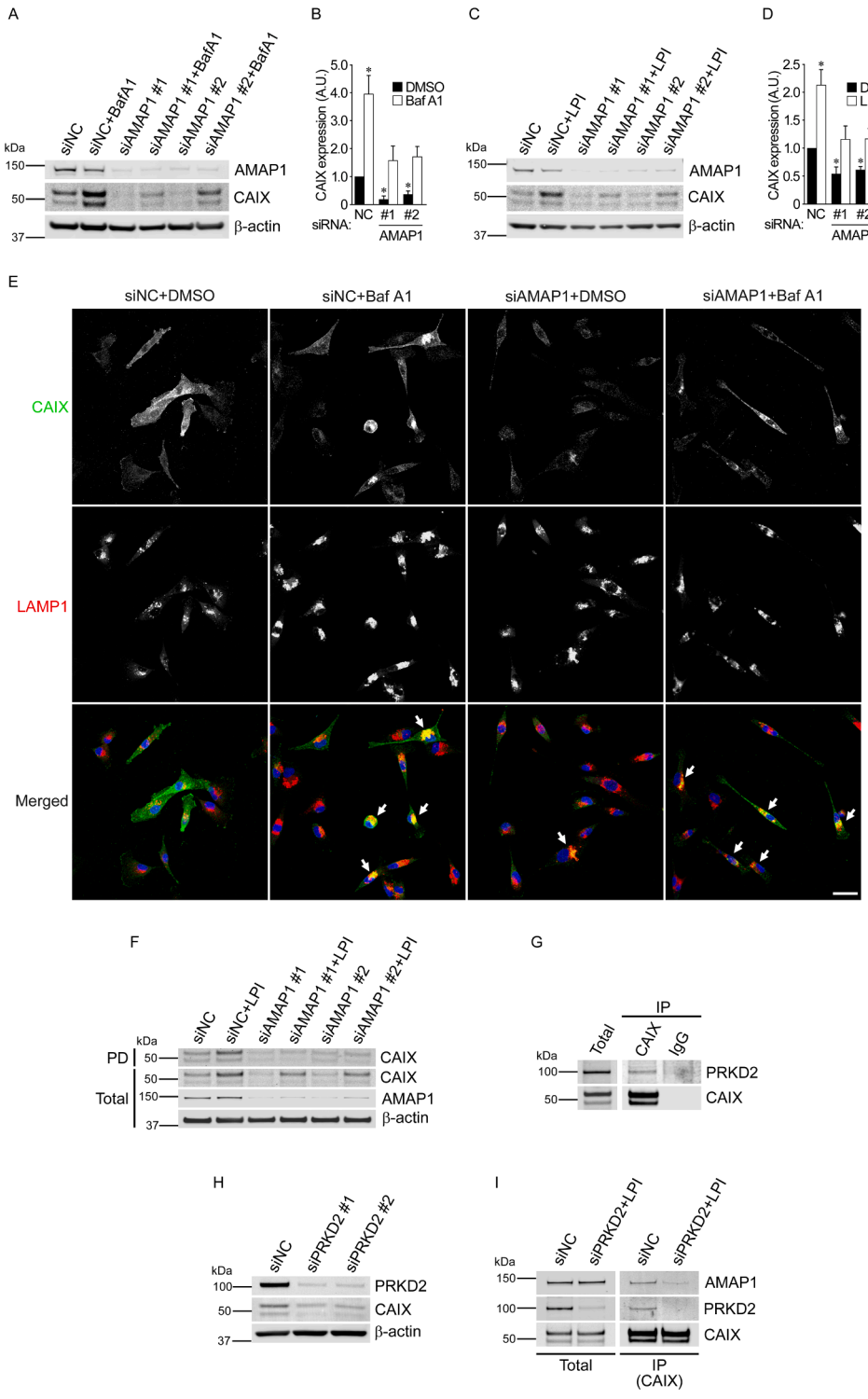

Fig. 2. Regulation of CAIX trafficking by the AMAP1-PRKD2 pathway.
(A–F) MDA-MB-231 cells were transfected with siRNAs targeting AMAP1 (siAMAP1) or negative control siRNA (siNC). Cells were pretreated with bafilomycin A1 (Baf A1, 100 nM, A,B), lysosomal protease inhibitors (LPI, 12.5 mM NH_4Cl and 0.5 mM leupeptin, C,D), or vehicles (DMSO or H_2O) for 24 h, and the cell lysates were analyzed by western blotting using the indicated antibodies (A and C). Expression levels of CAIX, normalized to those of β-actin (B and D). Cells transfected with siRNAs were treated with bafilomycin A1 (Baf A1) or vehicle (DMSO), and immunostained using CAIX (green) and LAMP1 (red) antibodies. Nuclei were also stained with Hoechst 33342 (blue). Arrows indicate the accumulation of CAIX in LAMP1-positive vesicles. Bar, 20 μm (E). Cells transfected with siRNAs were pretreated with LPI or vehicle (H_2O) for 24 h, and then surface-labeled with sulfo-NHS-SS-biotin. Biotinylated proteins were pulled down using NeutrAvidin beads (PD), and samples were analyzed by western blotting using the indicated antibodies (F). The CAIX protein complex was immunoprecipitated (IP) from MDA-MB-231 lysates. Nonimmune rabbit IgG was used as a control. Precipitants were analyzed by western blotting using the indicated antibodies (G). (H,I) MDA-MB-231 cells were transfected with siRNAs targeting PRKD2 (siPRKD2) or negative control siRNA (siNC). Cell lysates were analyzed by western blotting using the indicated antibodies (H). To equalize the expression level of CAIX, siRNA-transfected cells were pretreated with LPI (for siPRKD2) or H_2O (for siNC). CAIX was immunoprecipitated (IP), and precipitants were analyzed by western blotting using the indicated antibodies (I). All graphs indicate the mean ± SEM for at least 3 independent experiments. * and **, $P < 0.05$ and $P < 0.005$, compared to the control samples, respectively.

Interaction between CAIX and AMAP1 is mediated by PRKD2

PRKD2 binds to the cytoplasmic tail of β1-integrin and the proline-rich region of AMAP1, thus linking these 2 molecules [31]. PRKD2 was also found to be included in the CAIX protein complex (Fig. 2G). Furthermore, PRKD2-depleted cells demonstrated reduced CDIX protein levels (Fig. 2H), which was rescued by the inhibition of lysosomal degradation (see Fig. 2I), as was observed in AMAP1-depleted cells (see Fig. 2A–D). We then analyzed whether the AMAP1-CAIX association is mediated by PRKD2. PRKD2-depleted cells were treated with lysosomal inhibitors to maintain the protein level of CAIX. PRKD2 depletion indeed excluded AMAP1 from the CAIX protein complex (Fig. 2I), indicating that PRKD2 is required for the association of AMAP1 with CAIX. These data collectively suggest that CAIX trafficking is regulated together with β1-integrins via the AMAP1-PRKD2 pathway.

AMAP1 regulates CA9 transcription mediated by HIF-1α

As AMAP1 knockdown caused a substantial reduction in CAIX protein level, we speculated that *CA9* transcription was also affected in

some way. Indeed, quantification by qPCR showed that *CA9* mRNA level was significantly reduced by the knockdown of AMAP1 (Fig. 3A). HIF-1α plays a central role in the transcriptional regulation of *CA9* [21,22]. In some breast cancer cell lines, including MDA-MB-231, HIF-1α is stabilized by tumor-secreted metabolites even in normoxic conditions [40]. Intriguingly, the protein level of HIF-1α was significantly reduced by AMAP1 knockdown (Fig. 3B). The effects on HIF-1α mRNA level were different between the 2 AMAP1-targeting siRNAs (Fig. 3C), indicating that the reduced protein level was due to an alteration in protein stability. Indeed, the HIF-1α protein level was recovered by MG-132 (Fig. 3D), but not by lysosomal protease inhibitors (Supplementary Fig. 3), suggesting that the reduction in HIF-1α protein level by AMAP1 depletion is mediated by proteasomal degradation. We previously isolated AMAP1-binding proteins by yeast two-hybrid system [29], and one such protein, PIAS3, was reported to physically interact with HIF-1α to protect it from VHL-independent proteasomal degradation [41]. We confirmed the association of AMAP1 with PIAS3 by the GST-pulldown assay (Fig. 3E). The endogenous interaction of PIAS3 with AMAP1, as well as HIF-1α, was also observed in MDA-MB-231 cells (Fig. 3F). PIAS3 knockdown reduced the protein levels of HIF-1α and CAIX (Fig. 3G), the latter of which was associated with the decrease in its mRNA level (Fig. 3H). *HIF1A* mRNA was only slightly affected by PIAS3 knockdown (Fig. 3I). We then analyzed whether AMAP1 is essential for binding of PIAS3 to HIF-1α. AMAP1-depleted cells were pre-treated with MG-132 to maintain the protein levels of HIF-1α. In this condition, the level of PIAS3 was somehow decreased, whereas the level of HIF-1α was successfully maintained. Coprecipitation of HIF-1α was significantly decreased in AMAP1-depleted cells, even after taking into account of the difference in PIAS3 levels (Fig. 3J). These data suggest that the AMAP1-PIAS3 interaction is essential for PIAS3 binding to HIF-1α, which in turn stabilizes HIF-1α and thus promotes *CA9* transcription.

AMAP1 and PIAS3 cooperatively promote CAIX expression in breast cancer

To investigate whether the mode of action of the AMAP1-PIAS3 axis on HIF-1α and CAIX is common to various breast cancers, we also analyzed other highly invasive breast cancer cell lines, such as MDA-MB-436 and BT549, which have higher AMAP1 protein levels compared with low-invasive cell lines [29]. These 2 cell lines were also shown to have relatively high HIF-1α protein levels, even in normoxic conditions, similarly to MDA-MB-231 cells [40]. The knockdown of AMAP1 and PIAS3 significantly reduced protein levels of both HIF-1α and CAIX in MDA-MB-436 (Fig. 4A) and BT549 (Fig. 4B) cells, supporting the notion that a similar mechanism to that observed in MDA-MB-231 cells is indeed utilized among different breast cancer cell lines.

We then analyzed a transcriptome dataset of human breast cancer samples available at TCGA. The average *CA9* mRNA expression level was compared between the group with high *ASAP1* and/or *PIAS3* level (s), and the rest. The *ASAP1*-high group showed a relatively higher average *CA9* expression level compared with the rest or the samples, and the difference between the 2 groups reached a maximum when the threshold was set around the top 15% (Fig. 4C). On the other hand, the stratification by *PIAS3* expression alone showed the opposite tendency (Fig. 4D). However, intriguingly, the group with both high *ASAP1* (top 15%) and high *PIAS3* (top 12.5–50%) expression levels showed even higher average *CA9* levels (Fig. 4E). Average *ACTB* expression levels were almost constant among all of these stratifications (Supplementary Fig. 4A), indicating that the abovementioned tendencies are specific to *CA9*. Finally, we analyzed patients' prognoses using the same dataset.

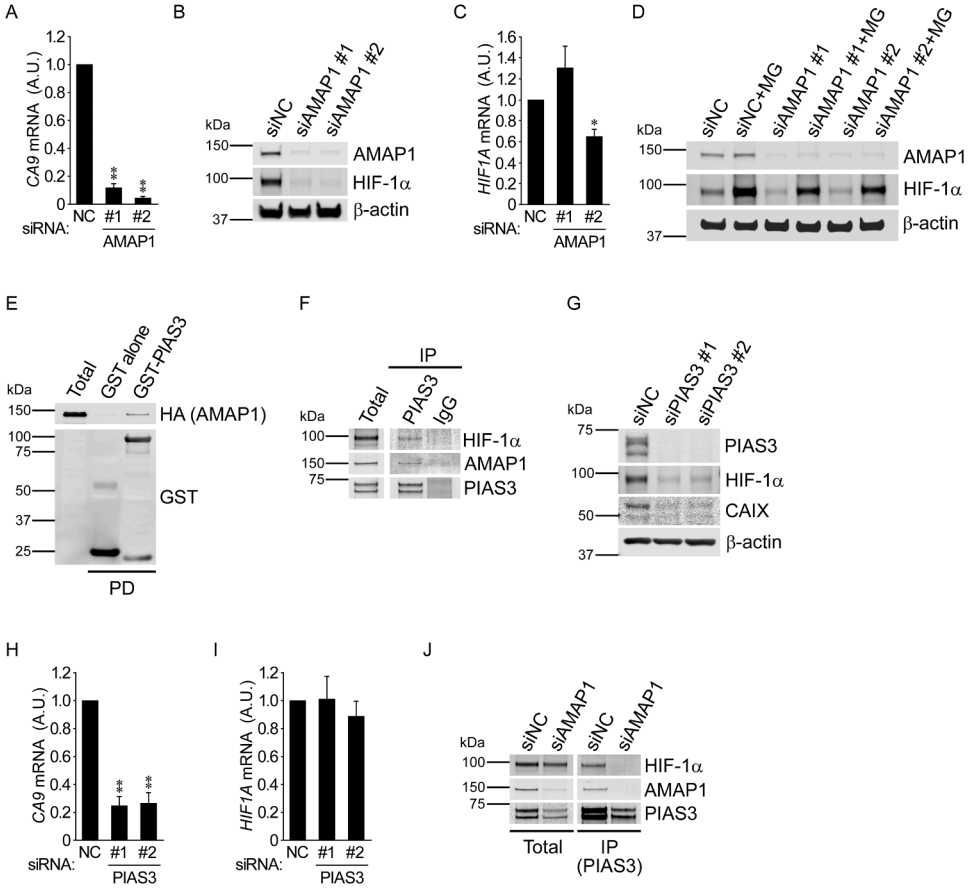

Fig. 3. AMAP1 regulates *CA9* transcription via PIAS3-mediated HIF-1α stabilization.
(A–D) MDA-MB-231 cells were transfected with siRNAs targeting AMAP1 (siAMAP1) or negative control siRNA (siNC). Cells were untreated (A–C), or pretreated with MG-132 (MG) or vehicle (DMSO) for 2 h (D). *CA9* (A) and *HIF1A* (C) mRNA levels, normalized by that of *ACTB*, were analyzed by qPCR. Cell lysates were analyzed by western blotting using the indicated antibodies (B and D). The GST-pulldown (PD) assay was performed using the crude lysate of 293T cells expressing AMAP1-HA and GST alone or GST-PIAS3 immobilized on glutathione beads. Precipitants were analyzed by western blotting using the indicated antibodies (E). PIAS3 was immunoprecipitated (IP) from MDA-MB-231 cell lysate. Nonimmune rabbit IgG was used as a control. Precipitants were analyzed by western blotting using the indicated antibodies. (G–I) MDA-MB-231 cells were transfected with siRNAs targeting PIAS3 (siPIAS3) or negative control siRNA (siNC). Cell lysates were analyzed by western blotting using the indicated antibodies (G). *CA9* (H) and *HIF1A* (I) mRNA levels, normalized by that of *ACTB*, was analyzed by qPCR. (J) MDA-MB-231 cells were transfected with siRNAs targeting AMAP1 (siAMAP1) or negative control siRNA (siNC). To equalize the expression level of HIF-1α, siRNA-transfected cells were pretreated with MG-132. PIAS3 was immunoprecipitated (IP), and precipitants were analyzed by western blotting using the indicated antibodies. All graphs indicate the mean ± SEM of at least 3 independent experiments. * and **, $P < 0.05$ and $P < 0.005$, compared to the control samples, respectively.

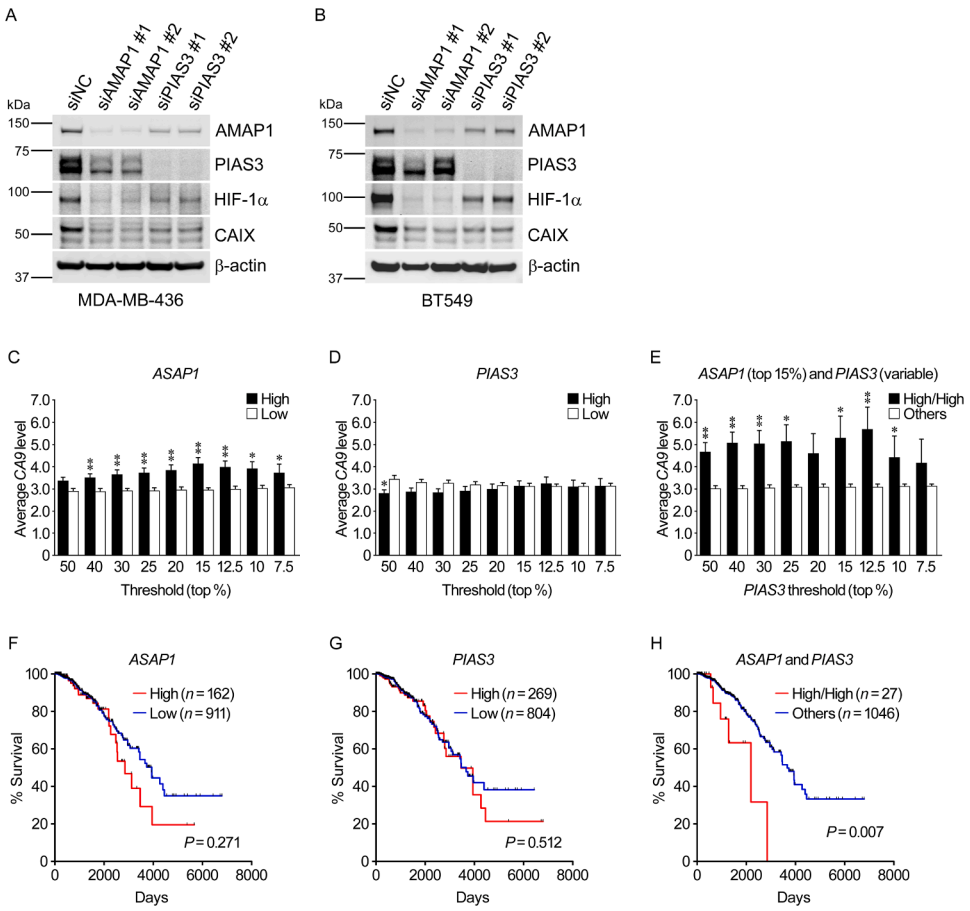

Fig. 4. Regulation of CAIX by the AMAP1-PIAS3 pathway in breast cancer.
(A–B) MDA-MB-436 (A) and BT549 (B) cells were transfected with siRNAs targeting AMAP1 (siAMAP1), PIAS3 (siPIAS3), or a negative control siRNA (siNC). Cell lysates were analyzed by western blotting using the indicated antibodies. (C—H) A TCGA dataset of breast cancer patients was stratified based on the expressions of *ASAP1* (C,F), *PIAS3* (D,G), or both (E,H). Quantification of average *CA9* level (C–E), and Kaplan-Meier survival analysis (F–H) were performed in each stratified group. All bar graphs indicate the mean ± SEM. * and **, $P < 0.05$ and $P < 0.005$, compared to the corresponding samples, respectively.

Similarly to previous analyses [42], high *CA9* expression correlated with a less favorable prognosis up to several years after diagnosis (Supplementary Fig. 4B). On the other hand, *ASAP1*-high (top 15%) or *PIAS3*-high (top 25%) alone did not show such a tendency (Fig. 4F,G). However, patients in the *ASAP1*-high (top 15%)/*PIAS3*-high (top 25%) group showed a significantly less favorable prognosis compared with the other groups (Fig. 4H). These results suggest that the cooperation between AMAP1 and PIAS3 is a crucial factor that reflects the prognosis of breast cancer patients, presumably in part by the regulation of CAIX.

Discussion

The molecular functions of CAIX are thought to be mainly based on its catalytic activity as a carbonic anhydrase [20,25], although many of its functions, including even pH regulation, do not necessarily involve its catalytic domain [16,37,43–45]. In any case, the roles of CAIX that have been described to date take place exclusively on the cell surface. On the other hand, the regulatory mechanisms of CAIX localization have not been studied in detail. In this study, we show that the cell-surface level of CAIX is largely regulated by the AMAP1-PRKD2 pathway, which promotes the recycling of β1-integrin to the plasma membrane in highly invasive breast cancer cells [31,35]. Swayampakula et al. reported that CAIX forms a protein complex with β1-integrins, and localizes at invadopodia to promote ECM degradation via local pH regulation [17]. In addition to the previous findings, the inclusion of both AMAP1 and PRKD2 in the CAIX protein complex, and the exclusion of AMAP1 from the complex by PRKD2 depletion (Figs. 1A, 2G,I) collectively indicate that CAIX trafficking is regulated together with β1-integrin via the AMAP1-PRKD2 pathway (Supplementary Fig. 5).

Knockdown of either AMAP1 or PRKD2 also induced the significant reduction of total CAIX level, which was partially rescued by the inhibition of lysosomal protein degradation. When control cells were treated with lysosomal inhibitors, the surface level of CAIX clearly increased (Fig. 2A–D), suggesting that the sorting of CAIX to late endosomes or lysosomes and its recycling back to the plasma membrane from these organelles take place in the steady state. Indeed, the CAIX-targeting antibody G250 was shown to be internalized by clathrin-mediated endocytosis, and to be at least partially recycled back to the plasma membrane in non-malignant MDCK cells [28]. Knockdown of AMAP1 significantly reduced the increase in surface CAIX level upon the inhibition of lysosomes, suggesting that the AMAP1 pathway is required for the recycling process. As CAIX-mediated pH-regulating functions require its localization on the cell surface, we speculate that the non-recycled, intracellularly-retained CAIX cannot take effects on cellular pH, although we did not analyze it considering direct effects on pH by the lysosomal inhibitors. The recycling back of integrins from lysosomes was reported to be regulated by Rab25 and CLIC3 [46]. It is worth investigating whether these proteins, as well as other proteins involved in integrin recycling [32–34,47], are also involved in the maintenance of surface CAIX level.

Investigation of the possible effects of AMAP1 on *CA9* transcription demonstrated the unexpected regulation of HIF-1α protein level, irrespective of the effects on its mRNA level, by AMAP1 (Fig. 3B). Our results collectively suggest that PIAS3 stabilizes the HIF-1α protein through its association with AMAP1, which in turn leads to the increased expression of CAIX (Supplementary Fig. 5). The cooperation of AMAP1 and PIAS3 in the transcriptional regulation of *CA9* was also supported by the analysis of the breast cancer dataset from TCGA (Fig. 4E). PIAS3 is well known as an inhibitor of active STAT3, and is often described as a suppressor of the malignant properties of various cancers [48]. Interestingly, although analysis of the TCGA dataset suggested that *PIAS3* expression on its own does not determine the outcome of breast cancers,

a high *PIAS3* expression level correlates well with an unfavorable prognosis when *ASAP1* expression is simultaneously high in a tumor (Fig. 4F,G). The stabilization of HIF-1α is known to potentiate the malignant properties of cancer cells through different mechanisms [49]. The unfavorable prognosis of *ASAP1*-high/*PIAS3*-high breast cancer might be in part owing to such HIF-1α-mediated effects, which does not necessarily involve CAIX. Indeed, this notion is partly supported by the fact that the prognosis of the *ASAP1*-high/*PIAS3*-high group was significantly less favorable than that of the *CA9*-high group (Fig. 4H and Supplementary Fig. 4B).

Whether the two-way roles of AMAP1 in the trafficking and transcription of CAIX are interconnected is also an important point. The AMAP1-PIAS3 association might be "sensing" the state of CAIX trafficking, which may reflect its usage, to provide feedback for its transcriptional regulation. The results of yeast two-hybrid screening using the AMAP1 proline-rich region [29], which successfully identified PIAS3 as an AMAP1-binding partner, suggested that AMAP1 in fact associates not only with CAIX but with variety of metabolic regulators on the cell surface, either directly or indirectly (data not shown). Interestingly, some such AMAP1-associated proteins are known to be regulated by the HIF-1 pathway, suggesting that they are also under dual regulation by AMAP1. The detailed molecular mechanisms by which the PIAS3-HIF-1α interaction is modulated by AMAP1 should be addressed elsewhere. Whether the molecular link between transcription and trafficking is a universal mechanism for the regulation of cell-surface proteins should also be investigated in the future.

The cancer-exclusive and hypoxia-inducible expression of CAIX has highlighted it as a promising and attractive target for cancer therapy. The noncatalytic, tumor-supportive roles of CAIX, however, suggest that its efficient targeting might require a multimodal approach, i.e., enzymatic inhibition alone by blocking the catalytic domain may not be sufficient. CAIX-targeting modalities, such as inhibitory antibodies, small molecules, and their drug conjugates (ADCs and SMDCs), are currently being developed [24–26]. The intracellular trafficking of their target proteins is known to greatly affect the efficacy of antibody-based modalities [27]. Importantly, human CAIX is cleaved on the cell surface by metalloproteinases [50]. Release of the cleaved ectodomain of CAIX proteins that are already bound to ADCs or SMDCs on the cell surface may impair the efficacy of these treatments. Therefore, inhibition of the trafficking machinery of CAIX may further enhance the effects of these treatment modalities by reducing the ectodomain cleavage, and may also become a new treatment strategy itself to block the CAIX-mediated malignant properties of cancer cells. The cooperative effects of blocking the AMAP1-PRKD2 pathway on these CAIX-targeting modalities should also be addressed in the future. At the same time, however, the possibility of the enhancement, rather than the reduction, of CAIX cleavage by blocking the AMAP1-PRKD2 pathway should be also carefully considered: the ectodomain cleavage may also be involved in the decrease in CAIX expression that occurs upon inhibition of the AMAP1-PRKD2 pathway.

Our data suggest that the blockade of AMAP1 is indeed effective to inhibit CAIX-mediated cellular pH regulation (Fig. 1I,J). Whereas AMAP1 expression is highly augmented in many cancer cells compared to the corresponding normal tissues [29,32,38], PRKD2 and PIAS3 are highly expressed in normal tissues as well and play essential roles which are not necessarily related to cancer [31,32,35,48]. Therefore, we do not expect that the blockade of PRKD2 or PIAS3 is suitable and/or effective for cancer therapy, even though their knockdown was also shown to effectively reduce CAIX expression (and probably its functions as well) by*in vitro* experiments (Figs. 2H, 3G). Development of AMAP1-targeting modality is also a key issue for the future.

CRediT authorship contribution statement

Mei Horikawa: Conceptualization, Visualization, Investigation, Data curation, Writing – original draft. **Hisataka Sabe:** Data curation, Writing – original draft. **Yasuhito Onodera:** Conceptualization, Visualization, Investigation, Data curation, Writing – original draft.

Declaration of Competing Interest

The authors declare that they have no known competing financial interests or personal relationships that could have appeared to influence the work reported in this paper.

Acknowledgements

This research was supported by JSPS KAKENHI Grant Number 18H02759, and a grant-in-aid from THE SUHARA MEMORIAL FOUNDATION (to Y.O.). We thank K. Kanno, and A. Oda for their assistance, and H. A. Popiel for her critical reading of the manuscript. The results published here are in part based upon data generated by the TCGA Research Network: https://www.cancer.gov/tcga.

Supplementary materials

Supplementary material associated with this article can be found, in the online version, at doi:10.1016/j.tranon.2021.101258.

References

[1] Y. Onodera, J.M. Nam, M.J. Bissell, Increased sugar uptake promotes oncogenesis via EPAC/RAP1 and O-GlcNAc pathways, J. Clin. Invest. 124 (2014) 367–384, https://doi.org/10.1172/JCI63146.
[2] N. Hay, Reprogramming glucose metabolism in cancer: can it be exploited for cancer therapy? Nat. Rev. Cancer 16 (2016) 635–649, https://doi.org/10.1038/nrc.2016.77.
[3] R.J. De Berardinis, N.S. Chandel, Fundamentals of cancer metabolism, Sci. Adv. 2 (2016), e1600200, https://doi.org/10.1126/sciadv.1600200.
[4] S.K. Parks, W. Mueller-Klieser, J. Pouysségur, Lactate and acidity in the cancer microenvironment, Annu. Rev. Cancer Biol. 4 (2020) 141–158, https://doi.org/10.1146/annurev-cancerbio-030419-033556.
[5] P. Swietach, What is pH regulation, and why do cancer cells need it? Cancer Metastasis Rev. 38 (2019) 5–15, https://doi.org/10.1007/s10555-018-09778-x.
[6] V. Huber, C. Camisaschi, A. Berzi, S. Ferro, L. Lugini, T. Triulzi, A. Tuccitto, E. Tagliabue, C. Castelli, L. Rivoltini, Cancer acidity: an ultimate frontier of tumor immune escape and a novel target of immunomodulation, Semin. Cancer Biol. 43 (2017) 74–89, https://doi.org/10.1016/j.semcancer.2017.03.001.
[7] S. Peppicelli, F. Bianchini, L. Calorini, Extracellular acidity, a "reappreciated" trait of tumor environment driving malignancy: perspectives in diagnosis and therapy, Cancer Metastasis Rev. 33 (2014) 823–832, https://doi.org/10.1007/s10555-014-9506-4.
[8] G. Hao, Z.P. Xu, L. Li, Manipulating extracellular tumour pH: an effective target for cancer therapy, RSC Adv. 8 (2018) 22182–22192, https://doi.org/10.1039/c8ra02095g.
[9] M. Flinck, S.H. Kramer, S.F. Pedersen, Roles of pH in control of cell proliferation, Acta Physiol. 223 (2018) e13068, https://doi.org/10.1111/apha.13068.
[10] D. Neri, C.T. Supuran, Interfering with pH regulation in tumours as a therapeutic strategy, Nat. Rev. Drug Discov. 10 (2011) 767–777, https://doi.org/10.1038/nrd3554.
[11] S.K. Parks, J. Chiche, J. Pouysségur, Disrupting proton dynamics and energy metabolism for cancer therapy, Nat. Rev. Cancer 13 (2013) 611–623, https://doi.org/10.1038/nrc3579.
[12] M. Damaghi, J.W. Wojtkowiak, R.J. Gillies, pH sensing and regulation in cancer, Front. Physiol. 4 (2013) 370, https://doi.org/10.3389/fphys.2013.00370.
[13] S. Pastorekova, R.J. Gillies, The role of carbonic anhydrase IX in cancer development: links to hypoxia, acidosis, and beyond, Cancer Metastasis Rev. 38 (2019) 65–77, https://doi.org/10.1007/s10555-019-09799-0.
[14] H.M. Becker, Carbonic anhydrase IX and acid transport in cancer, Br. J. Cancer 122 (2020) 157–167, https://doi.org/10.1038/s41416-019-0642-z.
[15] G. Venkateswaran, S. Dedhar, Interplay of carbonic anhydrase IX with amino acid and acid/base transporters in the hypoxic tumor microenvironment, Front. Cell Dev. Biol. 8 (2020) 1237, https://doi.org/10.3389/fcell.2020.602668.
[16] H.J. Shin, S.B. Rho, D.C. Jung, I.O. Han, E.S. Oh, J.Y. Kim, Carbonic anhydrase IX (CA9) modulates tumorassociated cell migration and invasion, J. Cell Sci. 124 (2011) 1077–1087, https://doi.org/10.1242/jcs.072207.
[17] M. Swayampakula, P.C. McDonald, M. Vallejo, E. Coyaud, S.C. Chafe, A. Westerback, G. Venkateswaran, J. Shankar, G. Gao, E.M.N. Laurent, Y. Lou, K. L. Bennewith, C.T. Supuran, I.R. Nabi, B. Raught, S. Dedhar, The interactome of metabolic enzyme carbonic anhydrase IX reveals novel roles in tumor cell migration and invadopodia/MMP14-mediated invasion, Oncogene 36 (2017) 6244–6261, https://doi.org/10.1038/onc.2017.219.
[18] E. Svastova, W. Witarski, L. Csaderova, I. Kosik, L. Skvarkova, A. Hulikova, M. Zatovicova, M. Barathova, J. Kopacek, J. Pastorek, S. Pastorekova, Carbonic

anhydrase IX interacts with bicarbonate transporters in lamellipodia and increases cell migration via its catalytic domain, J. Biol. Chem. 287 (2012) 3392–3402, https://doi.org/10.1074/jbc.M111.286062.
[19] A. Luong-Player, H. Liu, H.L. Wang, F. Lin, Immunohistochemical reevaluation of carbonic anhydrase IX (CA IX) expression in tumors and normal tissues, Am. J. Clin. Pathol. 141 (2014) 219–225, https://doi.org/10.1309/AJCPVJDS28KNYZLD.
[20] C.T. Supuran, V. Alterio, A. Di Fiore, K. D' Ambrosio, F. Carta, S.M. Monti, G. De Simone, Inhibition of carbonic anhydrase IX targets primary tumors, metastases, and cancer stem cells: three for the price of one, Med. Res. Rev. 38 (2018) 1799–1836, https://doi.org/10.1002/med.21497.
[21] S. Kaluz, M. Kaluzová, S.Y. Liao, M. Lerman, E.J. Stanbridge, Transcriptional control of the tumor- and hypoxia-marker carbonic anhydrase 9: a one transcription factor (HIF-1) show? Biochim. Biophys. Acta Rev. Cancer 1795 (2009) 162–172, https://doi.org/10.1016/j.bbcan.2009.01.001.
[22] G. De Simone, C.T. Supuran, Carbonic anhydrase IX: biochemical and crystallographic characterization of a novel antitumor target, Biochim. Biophys. Acta Proteins Proteom. 1804 (2010) 404–409, https://doi.org/10.1016/j.bbapap.2009.07.027.
[23] J. Pastorek, S. Pastorekova, Hypoxia-induced carbonic anhydrase IX as a target for cancer therapy: from biology to clinical use, Semin. Cancer Biol. 31 (2015) 52–64, https://doi.org/10.1016/j.semcancer.2014.08.002.
[24] S. Singh, C. Lomelino, M. Mboge, S. Frost, R. McKenna, Cancer drug development of carbonic anhydrase inhibitors beyond the active site, Molecules 23 (2018) 1045, https://doi.org/10.3390/molecules23051045.
[25] M.Y. Mboge, R. McKenna, S.C. Frost, Advances in Anti-cancer drug development targeting carbonic anhydrase IX and XII, Top. Anticancer Res. 5 (2015) 3–42, https://doi.org/10.2174/9781681083339116050004.
[26] S. Cazzamalli, A. Dal Corso, F. Widmayer, D. Neri, Chemically defined antibody- and small molecule-drug conjugates for *in vivo* tumor targeting applications: a comparative analysis, J. Am. Chem. Soc. 140 (2018) 1617–1621, https://doi.org/10.1021/jacs.7b13361.
[27] C. Chalouni, S. Doll, Fate of antibody-drug conjugates in cancer cells, J. Exp. Clin. Cancer Res. 37 (2018) 20, https://doi.org/10.1186/s13046-017-0667-1.
[28] M. Zatovicova, L. Jelenska, A. Hulikova, P. Ditte, Z. Ditte, L. Csaderova, E. Svastova, W. Schmalix, V. Boettger, P. Bevan, J. Pastorek, S. Pastorekova, Monoclonal antibody G250 targeting CA IX: binding specificity, internalization and therapeutic effects in a non-renal cancer model, Int. J. Oncol. 45 (2014) 2455–2467, https://doi.org/10.3892/ijo.2014.2658.
[29] Y. Onodera, S. Hashimoto, A. Hashimoto, M. Morishige, Y. Mazaki, A. Yamada, E. Ogawa, M. Adachi, T. Sakurai, T. Manabe, H. Wada, N. Matsuura, H. Sabe, Expression of AMAP1, an ArfGAP, provides novel targets to inhibit breast cancer invasive activities, EMBO J. 24 (2005) 963–973, https://doi.org/10.1038/sj.emboj.7600588.
[30] S. Hashimoto, Y. Onodera, A. Hashimoto, M. Tanaka, M. Hamaguchi, A. Yamada, H. Sabe, Requirement for Arf6 in breast cancer invasive activities, Proc. Natl. Acad. Sci. U. S. A. 101 (2004) 6647–6652, https://doi.org/10.1073/pnas.0401753101.
[31] Y. Onodera, J.M. Nam, A. Hashimoto, J.C. Norman, H. Shirato, S. Hashimoto, H. Sabe, Rab5c promotes AMAP1-PRKD2 complex formation to enhance β1 integrin recycling in EGF-induced cancer invasion, J. Cell Biol. 197 (2012) 983–996, https://doi.org/10.1083/jcb.201201065.
[32] Y. Onodera, J.M. Nam, H. Sabe, Intracellular trafficking of integrins in cancer cells, Pharmacol. Ther. 140 (2013) 1–9, https://doi.org/10.1016/j.pharmthera.2013.05.007.
[33] P. Moreno-Layseca, J. Icha, H. Hamidi, J. Ivaska, Integrin trafficking in cells and tissues, Nat. Cell Biol. 21 (2019) 122–132, https://doi.org/10.1038/s41556-018-0223-z.
[34] N.R. Paul, G. Jacquemet, P.T. Caswell, Endocytic trafficking of integrins in cell migration, Curr. Biol. 25 (2015) R1092–R1105, https://doi.org/10.1016/j.cub.2015.09.049.
[35] Y. Onodera, J.M. Nam, M. Horikawa, H. Shirato, H. Sabe, Arf6-driven cell invasion is intrinsically linked to TRAK1-mediated mitochondrial anterograde trafficking to avoid oxidative catastrophe, Nat. Commun. 9 (2018) 2682, https://doi.org/10.1038/s41467-018-05087-7.
[36] P.C. McDonald, S.C. Chafe, W.S. Brown, S. Saberi, M. Swayampakula, G. Venkateswaran, O. Nemirovsky, J.A. Gillespie, J.M. Karasinska, S.E. Kalloger, C. T. Supuran, D.F. Schaeffer, A. Bashashati, S.P. Shah, J.T. Topham, D.T. Yapp, J. Li, D.J. Renouf, B.Z. Stanger, S. Dedhar, Regulation of pH by carbonic anhydrase 9 mediates survival of pancreatic cancer cells with activated KRAS in response to hypoxia, Gastroenterology 157 (2019) 823–837, https://doi.org/10.1053/j.gastro.2019.05.004.
[37] M.Y. Mboge, Z. Chen, D. Khokhar, A. Wolff, L. Ai, C.D. Heldermon, M. Bozdag, F. Carta, C.T. Supuran, K.D. Brown, R. McKenna, C.J. Frost, S.C. Frost, A non-catalytic function of carbonic anhydrase IX contributes to the glycolytic phenotype and pH regulation in human breast cancer cells, Biochem. J. 476 (2019) 1497–1513, https://doi.org/10.1042/BCJ20190177.
[38] S. Hashimoto, S. Furukawa, A. Hashimoto, A. Tsutaho, A. Fukao, Y. Sakamura, G. Parajuli, Y. Onodera, Y. Otsuka, H. Handa, T. Oikawa, S. Hata, Y. Nishikawa, Y. Mizukami, Y. Kodama, M. Murakami, T. Fujiwara, S. Hirano, H. Sabe, ARF6 and AMAP1 are major targets of KRAS and TP53 mutations to promote invasion, PD-L1 dynamics, and immune evasion of pancreatic cancer, Proc. Natl. Acad. Sci. U. S. A. 116 (2019) 17450–17459, https://doi.org/10.1073/pnas.1901765116.
[39] V.W. Hsu, M. Bai, J. Li, Getting active: protein sorting in endocytic recycling, Nat. Rev. Mol. Cell Biol. 13 (2012) 323–328, https://doi.org/10.1038/nrm3332.
[40] K.J. Briggs, P. Koivunen, S. Cao, K.M. Backus, B.A. Olenchock, H. Patel, Q. Zhang, S. Signoretti, G.J. Gerfen, A.L. Richardson, A.K. Witkiewicz, B.F. Cravatt, J. Clardy, W.G. Kaelin, Paracrine induction of HIF by glutamate in breast cancer: EglN1 senses cysteine, Cell 166 (2016) 126–139, https://doi.org/10.1016/j.cell.2016.05.042.
[41] K. Nakagawa, T. Kohara, Y. Uehata, Y. Miyakawa, M. Sato-Ueshima, N. Okubo, M. Asaka, H. Takeda, M. Kobayashi, PIAS3 enhances the transcriptional activity of HIF-1α by increasing its protein stability, Biochem. Biophys. Res. Commun. 469 (2016) 470–476, https://doi.org/10.1016/j.bbrc.2015.12.047.
[42] Z. Chen, L. Ai, M.Y. Mboge, C. Tu, R. McKenna, K.D. Brown, C.D. Heldermon, S. C. Frost, Differential expression and function of CAIX and CAXII in breast cancer: a comparison between tumorgraft models and cells, PLoS ONE 13 (2018), e0199476, https://doi.org/10.1371/journal.pone.0199476.
[43] S. Jamali, M. Klier, S. Ames, L.F. Barros, R. McKenna, J.W. Deitmer, H.M. Becker, Hypoxia-induced carbonic anhydrase IX facilitates lactate flux in human breast cancer cells by non-catalytic function, Sci. Rep. 5 (2015) 1–16, https://doi.org/10.1038/srep13605.
[44] E. Švastová, N. Žilka, M. Zat'ovičová, A. Gibadulinová, F. Čiampor, J. Pastorek, S. Pastoreková, Carbonic anhydrase IX reduces E-cadherin-mediated adhesion of MDCK cells via interaction with β-catenin, Exp. Cell Res. 290 (2003) 332–345, https://doi.org/10.1016/S0014-4827(03)00351-3.
[45] M.Y. Mboge, J. Combs, S. Singh, J. Andring, A. Wolff, C. Tu, Z. Zhang, R. McKenna, S.C. Frost, Inhibition of carbonic anhydrase using SLC-149: support for a noncatalytic function of CAIX in breast cancer, J. Med. Chem. 64 (2021) 1713–1724, https://doi.org/10.1021/acs.jmedchem.0c02077.
[46] M.A. Dozynkiewicz, N.B. Jamieson, I. MacPherson, J. Grindlay, P.V. E. VandenBerghe, A. VonThun, J.P. Morton, C. Gourley, P. Timpson, C. Nixon, C. J. McKay, R. Carter, D. Strachan, K. Anderson, O.J. Sansom, P.T. Caswell, J. C. Norman, Rab25 and CLIC3 collaborate to promote integrin recycling from late endosomes/lysosomes and drive cancer progression, Dev. Cell 22 (2012) 131–145, https://doi.org/10.1016/j.devcel.2011.11.008.
[47] J.W. Hsu, M. Bai, K. Li, J.S. Yang, N. Chu, P.A. Cole, M.J. Eck, J. Li, V.W. Hsu, The protein kinase Akt acts as a coat adaptor in endocytic recycling, Nat. Cell Biol. 22 (2020) 927–933, https://doi.org/10.1038/s41556-020-0530-z.
[48] M. Wu, D. Song, H. Li, Y. Yang, X. Ma, S. Deng, C. Ren, X. Shu, Negative regulators of STAT3 signaling pathway in cancers, Cancer Manag. Res. 11 (2019) 4957–4969, https://doi.org/10.2147/CMAR.S206175.
[49] L. Schito, G.L. Semenza, Hypoxia-inducible factors: master regulators of cancer progression, Trends Cancer 2 (2016) 758–770, https://doi.org/10.1016/j.trecan.2016.10.016.
[50] M. Zatovicova, O. Sedlakova, E. Svastova, A. Ohradanova, F. Ciampor, J. Arribas, J. Pastorek, S. Pastorekova, Ectodomain shedding of the hypoxia-induced carbonic anhydrase IX is a metalloprotease-dependent process regulated by TACE/ADAM17, Br. J. Cancer 93 (2005) 1267–1276, https://doi.org/10.1038/sj.bjc.6602861.